Journal of Food Engineering 292 (2021) 110263

Contents lists available at ScienceDirect

Journal of Food Engineering

journal homepage: http://www.elsevier.com/locate/jfoodeng

Protective effect of carrier matrices on survival of *Lactobacillus plantarum* WCFS1 during single droplet drying explained by particle morphology development

I. Siemons [a,1], E.M.J. Vaessen [a,b,1], S.E. Oosterbaan van Peski [a,b], R.M. Boom [a], M.A. I. Schutyser [a,*]

[a] Laboratory of Food Process Engineering, Wageningen University and Research, P.O. Box 17 6700 AA, Wageningen, the Netherlands
[b] Food Microbiology, Wageningen University and Research, P.O. Box 17 6700 AA, Wageningen, the Netherlands

ARTICLE INFO

Keywords:
Spray drying
Glass transition
Lactic acid bacteria
Survival
Solute diffusion

ABSTRACT

Spray drying can be used to manufacture powder ingredients with lactic acid bacteria. Carrier matrices are used to increase survival of bacteria during drying; however, it is not exactly known why some matrices provide better protection than others. Depending on the carrier matrix and the drying conditions, different powder particle morphologies are obtained. Here, we employed single droplet drying to investigate the relation between particle morphology and survival of *Lactobacillus plantarum* WCFS1. Different carrier matrices with varying physico-chemical properties were selected and dried at 90 °C (R_0~100 μm), yielding smooth, hollow or dented morphologies. A clear correlation was observed between the observed particle morphologies and the viabilities after drying. Highest survival (78–90%) was obtained for dense and smooth particles; low survival (2–8%) was obtained for dented particles. The relation between the morphology and survival is likely to be rooted in a complex interplay between matrix properties and dynamics, where a skin that hinders evaporation most resulted in the highest inactivation. The identified correlation between morphology development and bacterial survival will be important to identify the mechanisms of inactivation of bacteria during drying.

1. Introduction

Lactic acid bacteria are widely used in food production as starter cultures or probiotics. These bacterial food ingredients are often dried and stored in the powder form to increase their shelf life (Broeckx et al., 2016; Huang et al., 2017; Peighambardoust et al., 2011). Freeze and spray drying are the main drying techniques that are used to industrially dry probiotics and starter cultures. Although during freeze drying the heat sensitive microorganisms are less exposed to heat as is the case during spray drying, spray drying is an interesting alternative since the drying time is shorter and the energy consumption is much smaller compared to freeze drying (Huang et al., 2017; Santivarangkna et al., 2007).

During spray drying, considerable inactivation of bacteria occurs due to thermal and dehydration stresses (Liu et al., 2018; Perdana et al., 2013). Therefore, bacteria are commonly dried in a protective matrix, consisting of for example carbohydrates, proteins or reconstituted skim milk to enhance their viability after drying (Broeckx et al., 2017; Perdana et al., 2014). The protective effect of these drying matrices, especially for sugars, is often explained by their ability to form a glassy matrix in which the cells are embedded and/or they may depress a phase change of the cellular membrane from liquid crystalline to gel phase (Broeckx et al., 2016; Leslie et al., 1995; Perdana et al., 2014). Additionally, the viability is also influenced by drying kinetics of the matrices, leading to a specific temperature-moisture content history of the droplets during drying (Ghandi, Powell, Chen and Adhikari, 2012b; Khem et al. 2015). In general, survival decreases considerably when the product is exposed to higher temperatures at higher moisture contents for a longer time (Liu et al., 2018; Perdana et al., 2013). The fact that some strategies lead to higher viability after spray drying shows that it is possible to increase the survival, though there is still a lack of insight in the reasons why some drying matrices result in better protection during spray drying compared to others.

Spray drying can yield entirely distinct particle morphologies

* Corresponding author.
E-mail address: maarten.schutyser@wur.nl (M.A.I. Schutyser).
[1] Shared first authorship: these authors contributed equally.

https://doi.org/10.1016/j.jfoodeng.2020.110263
Received 28 April 2020; Received in revised form 22 July 2020; Accepted 23 July 2020
Available online 12 August 2020

depending on the drying matrix and the applied drying conditions (e.g. smooth, hollow, dented) (Both et al., 2018; Siemons et al., 2020). Hitherto, particle morphology development during spray drying has been mainly studied with respect to physical powder properties such as bulk density and particle size (Both et al., 2018; Sadek et al., 2014; Schutyser et al., 2019). Some studies suggested that the development of the skin and the overall particle morphology during spray drying may also affect bacterial survival (Ghandi, Powell, Chen and Adhikari, 2012a; Khem et al. 2016; Khem et al., 2015; Wang et al., 2016). However, it is not known whether the particle morphology and bacterial survival can be linked. We here therefore hypothesize that the particle morphology as influenced by the properties of the carrier materials and drying conditions also has a specific effect on the survival of bacteria during spray drying.

In this study we focused on drying of sessile single droplets to evaluate this hypothesis. Sessile single droplet drying allows for drying of small droplets which can provide insight into spray drying processes when dried under well-controlled conditions (Schutyser et al., 2019). This method allows us to visually monitor the particle morphology development and analyze bacterial survival for each droplet after drying. Different drying matrices were selected (trehalose, xylose, whey proteins, maltodextrins) that lead to distinct particle morphologies and have different physicochemical properties (e.g. different glass transition temperatures). *Lactobacillus plantarum* WCFS1 was used as a model probiotic bacterium. A systematic set of experiments was conducted to distinguish between the direct effect of the matrix on the survival of bacteria, and the effect of morphology, indirectly influenced via the rheological properties of the matrix (Siemons et al., 2020). The results may contribute to the development of spray drying processes leading to higher bacterial survival.

2. Materials and methods

2.1. Carrier materials

Five types of drying matrices were investigated for their protective effects during drying of *L. plantarum* WCFS1 cells, i.e. whey protein, trehalose, maltodextrin dextrose equivalence (DE) 19, maltodextrin DE 5, and xylose. Whey proteins, purity 97.0–98.4% (BiPro®, Davisco, Switzerland), trehalose (Sigma Aldrich, USA), and xylose (Sigma Aldrich, USA) drying matrices were prepared at a dry matter concentration of 20% (w/w). The maltodextrin matrices (Roquette, France) had a dry matter concentration of 20% (w/w), 30% (w/w) or 40% (w/w) before drying. The protein matrices were stirred overnight at 4 °C to ensure complete hydration, while the carbohydrate matrices were stirred for a minimum of 30 min. All components were dissolved in demineralized water.

2.2. Microorganisms and pre-culture

Lactobacillus plantarum WCFS1 was obtained from the in-house strain collection. Pre-culture of this strain was performed according to the method described by Vaessen et al. (2018). *L. plantarum* WCFS1 was plated from a frozen stock on De Man, Rogosa and Sharpe (MRS) agar. The plates were incubated microaerobically at 30 °C for 60–70 h. After incubation, the plates were stored at 4 °C until further use. From these plates a single colony was transferred into 10 ml MRS broth and grown for 24 ± 2 h at 30 °C. This culture was subsequently diluted 1:100 into fresh MRS broth and incubated overnight for 17 ± 1 h at 30 °C. This overnight culture was centrifuged at 13,500×*g* for 10 min. The pH of the supernatant was measured to check the growth of the culture and was always 3.9 ± 0.1. The remaining pellet was washed once with a washing buffer (for composition see Vaessen et al. (2018)) and centrifuged again using the same settings. After centrifugation the supernatant was discarded and the pellet was suspended in the drying matrix. This culture in drying medium consisted of 3–4 · 10^9 CFU/ml.

2.3. Single droplet drying

The drying experiments were done using the single droplet drying equipment described earlier (Siemons et al., 2020). The droplets were dispensed by a PipeJet® NanoDispenser (BioFluidix, Germany) using 200-S PipeJet® Pipes (Biofluidix, Germany) on a flat hydrophobic membrane (Tetratex® ePTFE 3104 Polytetrafluoroethylene membrane, thickness 0.27 mm) (Donaldson Nederland B·V., The Netherlands). Droplets were dried for 20 s in a heated air flow from an insulated air feed tunnel (RH = 0%) at 90 °C, at a flow velocity of 0.3 m/s. Deposited droplets had an initial radius (R_0) of 100 ± 20 μm, which is roughly in the upper part of the droplet size range in industrial spray dryers (Filková et al., 2014). The size and shape were recorded with a camera. A complete overview (including pictures) of the setup can be found in Siemons et al. (2020). The obtained sequences were analyzed for the initial droplet size and locking point via image analysis using Image J software (National Institute of Health, USA). The locking point, which represents the onset of solidity and the morphology development, was defined as the first visual observation of shape deviation of the drying droplet during video analysis. The experiments were carried out in duplicate at least.

After drying, the particles were studied using scanning electron microscopy (SEM). For SEM analysis, samples were fixed on a sample holder using carbon adhesive tabs. SEM images were taken at 5 kV, 3.74 pA, using a Phenom G2 Pure SEM (Thermo Fischer Scientific, The Netherlands). For all droplets, a full image and a topographic image were made using a high sensitivity backscatter electron detector (Thermo Fischer Scientific, The Netherlands). The SEM analyses were performed at least in duplicate.

For each experiment with bacteria, first a droplet was dispensed and subsequently the membrane with the droplet was immediately transferred into a vial containing 1 ml phosphate buffered saline (PBS) for dissolution of the droplet. This was done at least in duplicate and these droplets served as the control, without drying. Additionally for each experiment two to six droplets were dried for 20 s at 90 °C. After drying, these droplets were kept on the membrane at room temperature for maximum 2 h until subsequent survival analysis. For each dispensed droplet the exact droplet volume was determined by stroboscopic images analyzed by the Biofluidix Control Software V2.9 (BioFluidix, Germany) and used for the calculation of the survival.

2.4. Survival analysis

The dried droplets were rehydrated by transferring the membrane with the dried droplet into vials containing 1 ml PBS. After at least 10 min of rehydration, this culture was decimally diluted by pipetting 50 μl of this rehydrated culture into 450 μl PBS. The control droplets, which were dispensed but not dried, were also decimally diluted in the same way. Subsequently, the diluted cultures were plated in duplicate on MRS agar plates and incubated for 48–96 h at 30 °C under microaerobic conditions. After incubation, the plates were counted and subsequently these counts were used to calculate the survival. Firstly, for each droplet the average CFU of the duplicate plates was used to calculate the CFU/nl of the initial droplet by taking into account the dilutions and the exact volume of the dispensed droplet. Secondly, the survival was calculated by dividing the average CFU/nl of the dried droplet by the average CFU/nl of the control droplets.

2.5. Experimental setup

All drying experiments with bacteria were carried out at least in duplicate, with each replicate being a fully independent experiment performed with another pre-culture and on another day. Additionally, for each experiment, multiple non-dried control and dried droplets were taken into account, to minimize the experimental errors. The morphology development during single droplet drying was also

evaluated for at least three droplets.

3. Results and discussion

3.1. Particle morphologies after single droplet drying

Trehalose, whey protein and maltodextrin DE19 solutions were dried at 90 °C using the sessile single droplet drying platform. In the initial phase of the drying process, the droplets decreased in size with similar rates, and remained spherical. After this initial drying phase, skin formation occurs due to an increased viscosity near the droplet surface. From the onset of the skin formation, often referred to as the locking point, the particle morphology starts to develop (Both et al., 2018; Siemons et al., 2020). In droplets with 20% (w/w) whey proteins we observed that an air vacuole started to develop shortly after the locking point (Fig. 1A). The final whey protein particle contained a large vacuole and had a smooth surface. The same morphology for whey protein particles was also observed in previous single droplet drying studies with droplets of a larger initial radius of ~500 μm at varying drying temperatures and whey protein concentrations (Both et al., 2018; Bouman, Venema, de Vries, van der Linden and Schutyser, 2016; Sadek et al., 2013). Also Khem et al. (2016) observed this morphology after spray drying of *Lactobacillus plantarum* in the presence of whey proteins. The droplets with 20% (w/w) trehalose shrank continuously until a small, dense and spherical particle was obtained (Fig. 1B). For trehalose no clear onset of skin formation could be observed. Droplets with 20% (w/w) maltodextrin DE19 formed a dented morphology (Fig. 1C), which resembled the morphology of dried maltodextrin DE21 as was described before by Siemons et al. (2020). In a spray drying study, Paramita et al. (2010) also found dented particles with high maltodextrin concentrations and smoother particles with high trehalose concentrations for mixtures of gum arabic and these components. Overall, the different final particle morphology types that we observed were a smooth dense particle, a smooth particle with a large vacuole and a dented particle.

To link the microbial survival after single droplet drying to the particle morphology, we selected components with different properties but leading to similar morphologies. For this purpose xylose, 20% (w/w) maltodextrin DE5 and 30% (w/w) maltodextrin DE5 were selected. Xylose is a monosaccharide that results in dense and smooth particles that are similar as those obtained with trehalose (Fig. 2). Drying of 20% (w/w) maltodextrin DE5 results in mostly dented particles, similar to maltodextrin DE19. However, maltodextrin DE19 had coarser edges and more smaller indentations, whereas maltodextrin DE5 had larger indentations with smoother edges (Fig. 2). Interestingly, when 30% (w/w) maltodextrin DE5 was dried, a particle with a large vacuole was formed, similar to the morphology of whey protein. For almost all of the drying matrices, we observed consistent development of similar morphology for each dried particle; only in few cases for 20% (w/w) maltodextrin DE5 a vacuole was observed similar to our observations for drying of 30% (w/w) maltodextrin DE5 (Fig. 2). Therefore, both types of morphologies are displayed in Fig. 2. Additional time series for all components can be found in the supplementary information (Fig. S1).

3.2. Survival of L. plantarum WCFS1

Survival of *Lactobacillus plantarum* WCFS1 after single droplet drying was evaluated for all drying matrices described in the previous section (Fig. 2). The survival was comparable for drying matrices that yielded similar particle morphologies (Fig. 3). The highest survival was observed with the matrices that yield dense smooth particles, namely xylose (90%) and trehalose (78%). The drying matrices that led to a smooth and hollow morphology resulted in moderate survival of 51% for whey proteins and 35% for 30% (w/w) maltodextrin DE5. Survival was lowest in drying matrices that resulted in dented particles, namely 2% for maltodextrin DE19 and 8% for 20% (w/w) maltodextrin DE5.

This lower survival for maltodextrin is in agreement with the study of Broeckx et al. (2017), who evaluated the survival of *L. rhamnosus* GG after spray drying, and found a higher survival with trehalose and lactose compared to maltodextrin DE6. Other studies reported a similar effect when comparing survival of *L. plantarum* WCFS1 in trehalose and maltodextrin (DE 19, DE 16 and 6) after spray drying (Perdana et al., 2014; Vaessen, den Besten, Leito and Schutyser, 2020). On the other hand, Vaessen et al. (2020) found a similar survival of *L. plantarum* WCFS1 in whey protein and trehalose after spray drying and Khem et al. (2015) found a higher survival of *Lactobacillus plantarum* A17 after single droplet drying in whey proteins compared to trehalose as drying matrix. This latter study ascribes this to the high temperature increase rates observed for trehalose droplets, while the temperature increase for whey protein droplets was more gradual. This is not in line with our observations. We speculate that the difference in drying conditions and drying time, e.g. 240 s in their study vs 20 s in our study, is relevant here.

The observed trends regarding survival of *L. plantarum* WCFS1 in the various drying matrices suggest that there is a relation between particle morphology development and survival of bacteria in this drying matrix. Though, before drawing further conclusions based on these observations, several aspects require further investigation. First of all, maltodextrin DE5 was used with two different concentrations; with a solids content of 20% (w/w) mainly a dented particle was formed, and with a solids content of 30% (w/w) a smooth particle with a large vacuole was formed. In line with the correlation that we found, the survival with 20%

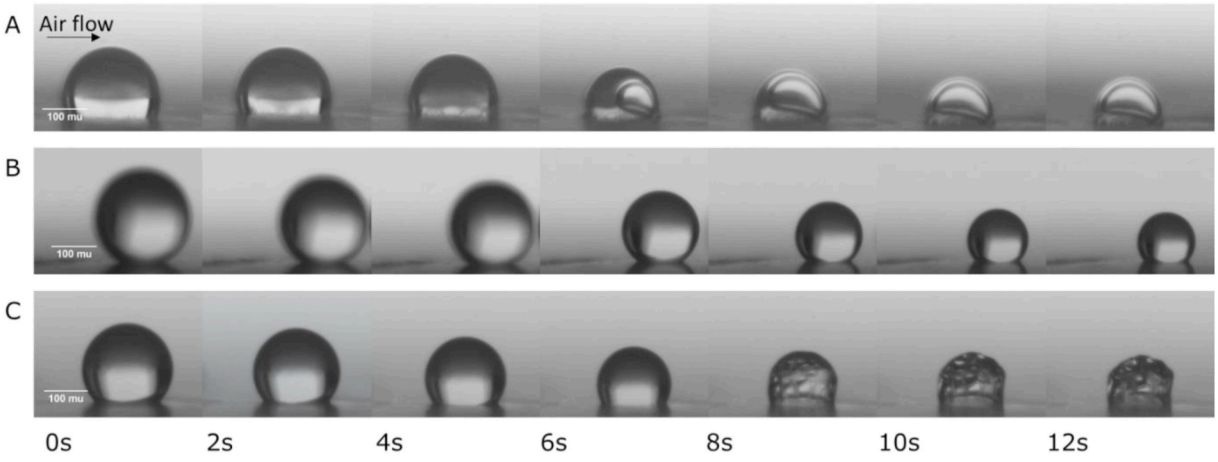

Fig. 1. Particle morphology development during single droplet dying at 90 °C of whey proteins (A), trehalose (B) and maltodextrin DE19 (C) at 20% (w/w) initial solids concentration, R_0 100 ± 20 μm (mu indicates μm). Air flow came from the left as indicated in the figure by the arrow.

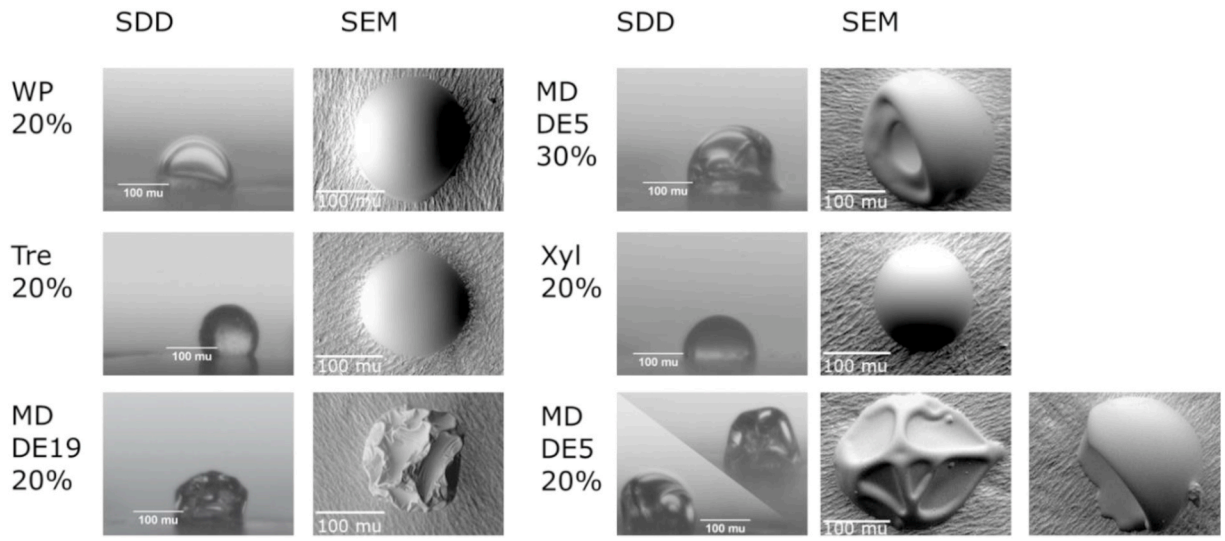

Fig. 2. Final particle morphologies after single droplet drying at 90 °C of various drying matrices. WP = whey proteins, Tre = trehalose, MD DE19 = maltodextrin DE19, Xyl = xylose, MD DE5 = maltodextrin DE5. The initial solids concentrations are indicated in percentages and scale bars are provided.

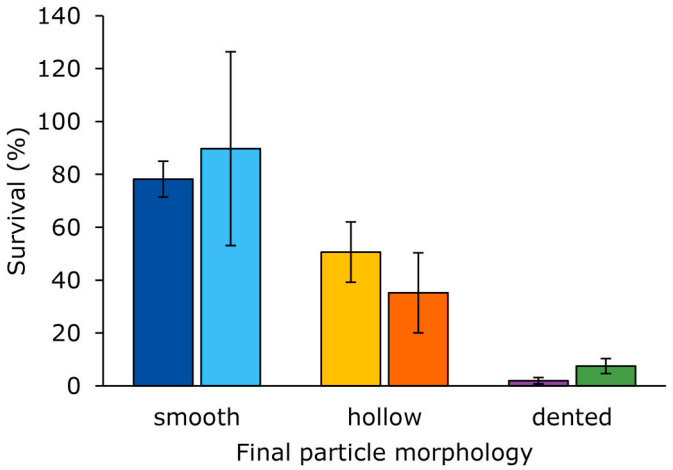

Fig. 3. Survival of *L. plantarum* WCFS1 after single droplet drying at 90 °C in various drying matrices. The drying matrices were (from left to right): 20% (w/w) trehalose (dark blue), 20% (w/w) xylose (light blue), 20% (w/w) whey proteins (yellow), 30% (w/w) maltodextrin DE5 (orange), 20% (w/w) maltodextrin DE19 (purple) and 20% (w/w) maltodextrin DE5 (green). Error bars represent standard deviations of independent replicates (n ≥ 2). (For interpretation of the references to colour in this figure legend, the reader is referred to the Web version of this article.)

DE5 was low, while the survival with 30% was moderate. This means that the same type of drying matrix with different morphology gives different survival.

3.3. Effect of solids content and duration of constant rate period

We evaluated the survival of *L. plantarum* WCFS1 in maltodextrin DE19 and maltodextrin DE5 as drying matrices at various solids contents. Survival in maltodextrin DE5 increased from 8% to 35% with increasing solids content from 20% (w/w) to 30% (w/w) and changing morphology from predominantly dented to hollow (Fig. 2). For maltodextrin DE19 the increase in survival from 2% to 5% was not significant with the same increase in solids content (Fig. 4A). Further increasing the solids content to 40% (w/w) resulted in a slightly higher survival of 13%. For all of these matrices we found dented particle morphologies (Fig. 4B), where only the edges and indentations of the particles became less coarse upon increasing the initial solids content. Unfortunately, it was not possible to dry maltodextrin DE5 at 40% (w/w) as the viscosity was already too high for dispensing.

In literature, different effects of solids content have been reported for survival of bacteria after drying. For example, Perdana et al. (2014) found that 2% (w/w) trehalose was sufficient to protect *L. plantarum* WCFS1 during drying, and found no further increase in survival by increasing the trehalose content further. Another study reported that increasing the content of gelatin, gum arabic or soluble starch from 10 to 20 and 30% (w/w) resulted in a lower survival of Bifidobacteria compared to 10% (w/w) (Lian et al., 2002). On the other hand, Ghandi et al. (2012a) reported an increase in survival of *Lacotococcus lactis* when this strain was dried at higher solids contents. For example, the survival increased from 9 to 22% when increasing the solids content of a lactose-sodium caseinate carrier from 10 to 35% (w/w). Würth et al. (2018) described a decrease in survival of *L. paracasei* when increasing the solids content of a skim milk concentrate from 12.5% (w/w) to 35% (w/w). Important to note is that all the previous authors kept the amount of bacteria in the feed solution constant, whereas Würth et al. (2018) kept the biomass to solids ratio constant. Additionally, they found a strong correlation between the particle size of the spray dried particle and bacterial survival; a smaller particle resulted in better survival. They relate this to the solids content, with lower solids contents leading to a smaller final particle and a prolonged constant rate period (Würth et al., 2018). To evaluate whether the duration of this constant rate drying period can be linked to survival, we used the locking point as measure for the duration of the constant rate drying period (Fig. 5).

The determination of the locking point was based on the visual analysis of droplet drying videos. At the locking point, the spherical shape of the droplet becomes distorted and shows first signs of cavity formation or denting (Siemons et al., 2020). The droplets with trehalose and xylose did not exhibit a clear locking point. These droplets have a longer constant rate period (Supplementary information, Fig. S2), and did not show any distortions from spherical shape, eventually resulting in small spherical particles. This was expected as for these small sugars the solute diffusivity is faster or comparable to the drying rate (Vehring, 2008; Vehring et al., 2007). Therefore, the saturation at the droplet surface is reached late in the drying process with relatively homogeneous distribution of these sugars in the droplet. Overall, we did not observe a consistent relation between the locking point time, i.e. the duration of the constant rate period and the survival of *L. plantarum* WCFS1 after drying (Fig. 5).

Several single droplet drying studies described that the inactivation

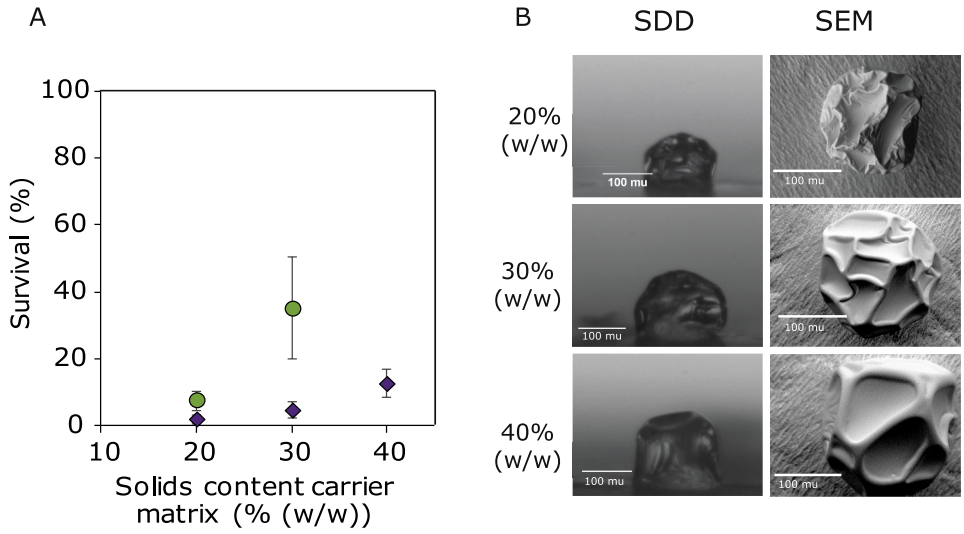

Fig. 4. Effect of solids content on survival of *L. plantarum* WCFS1 (A) and particle morphology (B). (A) Survival of *L. plantarum* WCFS1 in maltodextrin DE19 (purple diamonds) and maltodextrin DE5 (green circles). Error bars indicate standard deviations of independent replicates (B) Final particle morphologies after single droplet drying at 90 °C of maltodextrin DE19 at various solids content, i.e. 20, 30 and 40% (w/w). Scale bars representing 100 μm are provided (mu indicates μm). (For interpretation of the references to colour in this figure legend, the reader is referred to the Web version of this article.)

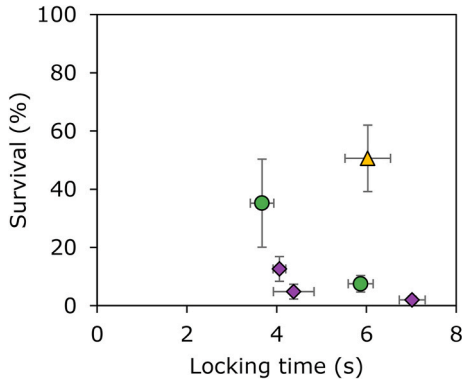

Fig. 5. Survival of *L. plantarum* WCFS1 after single droplet drying in several drying matrices as a function of the locking time. The drying matrices are whey proteins (yellow triangle), maltodextrin DE5 (green circles) and maltodextrin DE19 (purple diamonds). Horizontal error bars represent the standard error of the locking point analysis and vertical error bars represent the standard deviation of bacterial survival. The matrices with trehalose and xylose did not exhibit a clear locking point. (For interpretation of the references to colour in this figure legend, the reader is referred to the Web version of this article.)

during the constant rate period is limited, probably due to the low droplet temperature (wet bulb temperature) during this period. These studies show that most inactivation took place during the second, falling rate period of drying (Khem et al., 2015; Zheng et al., 2015). In this period, diffusion limitation is dominant and the droplet temperature increases gradually towards the air temperature. If this happens when the droplet is still high in water internally, this will result in strong thermal inactivation. Therefore, it is expected that the microbial survival rate is more strongly coupled to the processes in the falling rate period, than it is to processes in the constant rate period.

3.4. Effect of physicochemical matrix properties

The physical state of the matrix during drying, i.e. glassy or non-glassy, is considered important to the survival of probiotics during and after drying (Santivarangkna et al., 2011). As the evaporation of water progresses during drying, the viscosity of the droplet surface will increase until the surface reaches a critical temperature and moisture content, at which the matrix will behave as a glass. The extremely high viscosity of amorphous glassy matrices ($\geq 10^{12}$ Pa s) effectively halts diffusion-controlled deterioration reactions, improving the chemical and physical stability of the embedded bacterial cells (Aschenbrenner et al., 2012; Schutyser et al., 2012).

Carrier materials with a high glass transition temperature (T_g) are expected to provide a glassy matrix earlier during droplet drying or soon after drying upon cooling (Perdana et al., 2012, 2014). We estimated the T_g as function of moisture content for every component studied in this work using the Couchman-Karasz theory (Fig. 6A). This theory is further explained in the Appendix (Table A.1,Eqn A.1).

Maltodextrin DE5 has the highest T_g for moisture contents below 0.3 kg water/kg, followed by maltodextrin DE19 and trehalose, whey proteins and xylose (Fig. 6A). In Fig. 6B the survival is given as function of the T_g of the anhydrous matrix. Fig. 6B indicates that a higher T_g of a matrix is not directly correlated to higher retention of viability after drying. In particular, the survival percentages found for *L. plantarum* WCFS1 after drying in maltodextrin and xylose matrices contradict the hypothesis that matrices with high T_g offer higher degree of survival after drying. The relation between morphology development and survival is more likely rooted in a complex interplay between matrix properties and drying kinetics.

While entering the glassy state at an early stage during drying in principle should offer better survival, it also halts the drying process itself by reducing the water diffusivity (Ribeiro et al., 2002; Zobrist et al., 2011). For maltodextrin matrices, it is expected that the skin that is formed upon concentration will quickly move towards the glass transition, where the viscosity increases dramatically, and water diffusivity is strongly reduced. The decreased water diffusivity causes the droplet temperature to increase, while the viscosity of the skin remains high due to ongoing evaporation. The relatively fast skin formation followed by a quick approach of the glassy state may result in a short constant rate period, and a quickly rising droplet temperature, while the droplet interior may still have relatively high water content. Especially the combination of elevated temperature and high moisture content may lead to extensive microbial inactivation.

Whey proteins undergo a colloidal glass transition already above a solids concentration of 50% (w/w) (Both et al., 2019a; Both et al., 2019b). This transition is based on jamming, leading to elasticity, and not just an increase in viscosity. Therefore, as soon as the skin is formed, it will withstand the surface stresses and retains its shape, while at the same time lower internal pressures develop due to the ongoing evaporation (Both et al., 2018; Bouman et al., 2016). At some point, a weak point in the skin will yield, and a cavity is formed. In this case, the glassy colloidal skin does not directly result in quickly rising droplet temperatures, since the cavity serves as an evaporation vent (Bouman et al.,

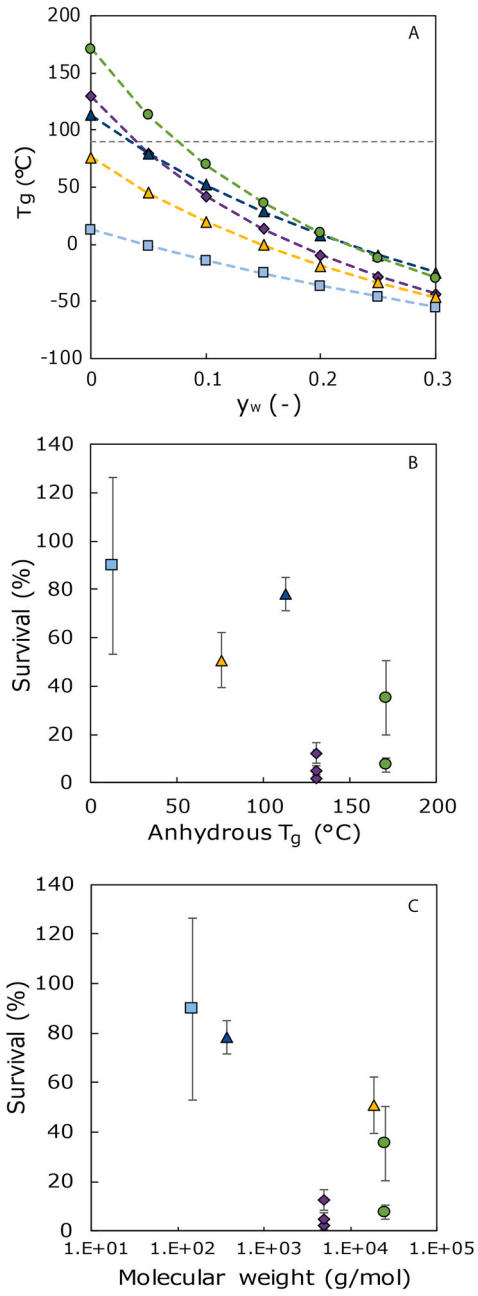

Fig. 6. (A) Glass transition temperatures as function of moisture content (y_w) as calculated with Couchman-Karasz. The drying air temperature of 90 °C is indicated with a dotted line. (B) Survival of *L. plantarum* WCFS1 after single droplet drying as function of anhydrous glass transition temperature and (C) as a function of the molecular weight. The components are trehalose (blue triangles), xylose (light blue squares), whey proteins (yellow triangles), maltodextrin DE5 20 and 30% (w/w) (green circles) and maltodextrin DE19 20, 30 and 40% (w/w) (purple diamonds). (For interpretation of the references to colour in this figure legend, the reader is referred to the Web version of this article.)

2016). Therefore, the droplet temperature and moisture profiles during drying may be different from the dented maltodextrin droplet as described before. Hence, bacteria may be better protected against heat and high moisture content due to prolonged constant drying via the cavity. It may even be that the vacuole formation causes a longer constant rate period than what was predicted based on locking point analysis. The latter might also explain higher survival for maltodextrin DE5 at 30% (w/w).

Trehalose is a disaccharide, while xylose is a monosaccharide. These molecules have relative high diffusivities compared to oligo- or polysaccharides (van der Sman and Meinders, 2013). Therefore, these components will accumulate more slowly below the surface, and the droplet will lose more of its moisture in the constant rate regime, where the temperature is low and microbial inactivation is therefore limited. Indeed we observed via image analysis that the constant rate regime continued for a longer time with these matrices (Supplementary information, Fig.S2). These droplets only come into the falling rate period at a later stage, when the concentration of water has reduced strongly. The latter implies that the period of microbial inactivation has shortened, and the lower water content at the start of the falling rate period may additionally slow down the inactivation.

On the cellular level, the protective effect of low molecular weight carbohydrates such as trehalose and xylose is often explained by their ability to depress the phase transition of the bacterial cell membrane due to interactions with the phospholipids (Bryant et al., 2001; Huang et al., 2017). Indeed, the low molecular weight components in our experiments provided the best protection during survival (Fig. 6C). However, at higher molecular weights no relationship is observed between molecular weight and bacterial survival in this matrix. This differs from Perdana et al. (2014), who observed a decreasing residual viability with increasing molecular weight if the molecular weight was higher than $2{\cdot}10^3$ g/mol. A complication in this comparison of survival and molecular weight is that maltodextrins are mixtures of smaller and larger carbohydrates, especially maltodextrin DE19 contains a considerable amount of low molecular weight components (Avaltroni et al., 2004). In addition to the importance of low molecular weight, the combination of low molecular weight and glass transition is also often described as an important aspect for the stabilization of bacterial cell membranes. Glass transition close to the membrane phospholipids might reduce the compressive stresses that force the membrane lipids from a fluid phase into a gel phase causing loss of membrane integrity (Bryant et al., 2001). For this effect components should be small enough to enter the spacing between membranes and have a high T_g. Actually, this is not in agreement with the high survival of xylose, which has a very low glass transition temperature (Fig. 6A and B). Despite the possible capability of xylose to enter the intermembrane spacing due to its low molecular weight, it is still likely that xylose does not vitrify during drying as the T_g values are far below the drying air temperature. This might also affect survival during storage after drying, which is of great importance for dried bacterial ingredients and requires further investigation since it has not been considered in our study.

We demonstrate that the clear relation that we found between the morphology and the microbial survival, is likely rooted in a complex interplay between matrix properties (glass transition) and drying dynamics (diffusion rates). However they are both the consequence of the same process; hence the strong correlation between these two resultants. This implies that the investigation of the morphologies may well offer a route towards better microbial survival during spray drying.

4. Conclusions and outlook

Drying of droplets having different matrices resulted in smooth, hollow or dented particles. Dented or folded particles were developed for maltodextrin DE19 and 20% (w/w) maltodextrin DE5; hollow particles were observed for whey protein and 30% (w/w) maltodextrin DE5, while smooth spherical and dense particles were obtained for trehalose and xylose. The survival of *Lactobacillus plantarum* WCFS1 that was embedded in these matrices showed clear correlation with these morphologies, with the smooth particles giving high survival, dented particles low survival, and hollow particles in between.

This strong correlation can be explained by a combination of drying dynamics and the glass transition, with high-molecular weight components like maltodextrins giving fast formation of a viscous shell, which folds into a dented geometry, allowing significant inactivation due to the

long falling rate period at elevated temperatures. Small components such as xylose and trehalose exhibit a much longer constant rate period, and significant protection against inactivation during the shorter falling rate period. The hollow particles are the result of an elastic shell that resists folding, but offer a prolonged constant evaporation due to cavity formation allowing fast evaporation and therefore a longer low temperature period than the high-molecular weight maltodextrins.

Our results suggest that the morphology development is strongly correlated to the microbial survival, because it is fundamentally related to the same underlying mechanisms. Therefore it is an excellent phenomenon to use for optimizing microbial survival during spray drying.

Other bacterial strains and different drying matrices, including mixes of carbohydrates and proteins, should be tested to further support our findings. Single sessile droplet drying experiments offer the opportunity to probe many bacterial drying formulations and drying conditions to find promising particle morphologies leading to higher bacterial survival.

CRediT authorship contribution statement

I. Siemons: Conceptualization, Methodology, Investigation, Formal analysis, Writing - original draft. **E.M.J. Vaessen:** Conceptualization, Methodology, Investigation, Formal analysis, Writing - original draft. **S. E. Oosterbaan van Peski:** Methodology, Investigation. **R.M. Boom:** Conceptualization, Writing - review & editing. **M.A.I. Schutyser:** Funding acquisition, Conceptualization, Supervision, Writing - review & editing.

Declaration of competing interest

The authors declare that they have no known competing financial interests or personal relationships that could have appeared to influence the work reported in this paper.

Acknowledgements

This research is supported by the Netherlands Organization for Scientific Research (NWO) (grant number 15459) and has also been carried out in the framework of an Institute for Sustainable Process Technology (ISPT) project (DR-20-06).

Appendix A. Supplementary data

Supplementary data to this article can be found online at https://doi.org/10.1016/j.jfoodeng.2020.110263.

Appendix. Glass transition temperatures and molecular weights

In our study, the glass transition temperature T_g of the different components was estimated as a function of moisture content. The relation was described using the theory of Couchman and Karasz (1978):

$$T_g = \frac{y_w \Delta c_{P,w} T_{g,w} + y_s \Delta c_{p,s} T_{g,s}}{y_w \Delta c_{p,w} + y_s \Delta c_{p,s}} \quad (A.1)$$

Here $y_i$is the mass fraction ($i = w, s$ for water and solute), $T_{g,i}$is the glass transition temperature for the pure component ($T_{g,w}$=139 K), $\Delta c_{p,i}$ is the change in the specific heat at the glass transition. For $\Delta c_{p,w}$a value of 1.91 kJ/kg·K was used. Glass transition temperatures of maltodextrins were determined as described by (Siemons et al., 2020). The anhydrous glass transition temperature and the heat capacities of the solutes and the molecular weights of the components are provided in Table A1.

Table A.1
Overview of materials and their anhydrous glass transition temperature, specific heat capacity and molecular weight.

Pure components	T_g (°C)	Δc_p (J·g^{-1}K^{-1})	Mw (g·mol^{-1})	Reference
Trehalose	113	0.65	342	Kawai et al. (2005)
Xylose	13	0.95	150	Kalichevsky et al. (1993)
Whey proteins	76	0.58	18,200	(Nicolai et al., 2011; Yang et al., 2010)
Maltodextrin DE19	130	0.43	4978	(Castro et al., 2016; Van Der Sman &; Meinders, 2011)
Maltodextrin DE5	171	0.43	25,847	(Castro et al., 2016; Van Der Sman &; Meinders, 2011)

References

Aschenbrenner, M., Kulozik, U., Foerst, P., 2012. Evaluation of the relevance of the glassy state as stability criterion for freeze-dried bacteria by application of the Arrhenius and WLF model. Cryobiology 65 (3), 308–318. https://doi.org/10.1016/j.cryobiol.2012.08.005.

Avaltroni, F., Bouquerand, P.E., Normand, V., 2004. Maltodextrin molecular weight distribution influence on the glass transition temperature and viscosity in aqueous solutions. Carbohydr. Polym. 58 (3), 323–334. https://doi.org/10.1016/j.carbpol.2004.08.001.

Both, E.M., Karlina, A.M., Boom, R.M., Schutyser, M.A.I., 2018. Morphology development during sessile single droplet drying of mixed maltodextrin and whey protein solutions. Food Hydrocolloids 75, 202–210. https://doi.org/10.1016/j.foodhyd.2017.08.022.

Both, E.M., Siemons, I., Boom, R.M., Schutyser, M.A.I., 2019a. The role of viscosity in morphology development during single droplet drying. Food Hydrocolloids 94, 510–518. https://doi.org/10.1016/j.foodhyd.2019.03.023.

Both, E.M., Tersteeg, S.M.B., Boom, R.M., Schutyser, M.A.I., 2019b. Drying kinetics and viscoelastic properties of concentrated thin films as a model system for spray drying. Colloid. Surface. Physicochem. Eng. Aspect. 585 https://doi.org/10.1016/j.colsurfa.2019.124075.

Bouman, J., Venema, P., de Vries, R.J., van der Linden, E., Schutyser, M.A.I., 2016. Hole and vacuole formation during drying of sessile whey protein droplets. Food Res. Int. 84, 128–135. https://doi.org/10.1016/j.foodres.2016.03.027.

Broeckx, G., Vandenheuvel, D., Claes, I.J.J., Lebeer, S., Kiekens, F., 2016. Drying techniques of probiotic bacteria as an important step towards the development of novel pharmabiotics. Int. J. Pharm. 505 (1–2), 303–318. https://doi.org/10.1016/j.ijpharm.2016.04.002.

Broeckx, G., Vandenheuvel, D., Henkens, T., Kiekens, S., van den Broek, M.F.L., Lebeer, S., Kiekens, F., 2017. Enhancing the viability of *Lactobacillus rhamnosus* GG after spray drying and during storage. Int. J. Pharm. 534 (1–2), 35–41. https://doi.org/10.1016/j.ijpharm.2017.09.075.

Bryant, G., Koster, K.L., Wolfe, J., 2001. Membrane behaviour in seeds and other systems at low water content: the various effects of solutes. Seed Sci. Res. 11 (1), 17–25. https://doi.org/10.1079/SSR200056.

Castro, N., Durrieu, V., Raynaud, C., Rouilly, A., 2016. Influence of DE-value on the physicochemical properties of maltodextrin for melt extrusion processes. Carbohydr. Polym. 144, 464–473. https://doi.org/10.1016/j.carbpol.2016.03.004.

Couchman, P.R., Karasz, F.E., 1978. A classical thermodynamic discussion of the effect of composition on glass-transition temperatures. Macromolecules 11 (1), 117–119. https://doi.org/10.1021/ma60061a021.

Filková, I., Huang, L.X., Mujumdar, A.S., 2014. Industrial spray drying systems. Handbook of Industrial Drying.

Ghandi, A., Powell, I.B., Chen, X.D., Adhikari, B., 2012a. The effect of dryer inlet and outlet air temperatures and protectant solids on the survival of *Lactococcus lactis* during spray drying. Dry. Technol. 30 (14), 1649–1657. https://doi.org/10.1080/07373937.2012.703743.

Ghandi, A., Powell, I., Chen, X.D., Adhikari, B., 2012b. Drying kinetics and survival studies of dairy fermentation bacteria in convective air drying environment using single droplet drying. J. Food Eng. 110 (3), 405–417. https://doi.org/10.1016/j.jfoodeng.2011.12.031.

Huang, S., Vignolles, M.-L., Chen, X.D., Loir, Y. Le, Jan, G., Schuck, P., Jeantet, R., 2017. Spray drying of probiotics and other food-grade bacteria : a review. Trends Food Sci. Technol. 63, 1–17. https://doi.org/10.1016/j.tifs.2017.02.007 0924-2244/©.

Kalichevsky, M.T., Jaroszkiewicz, E.M., Blanshard, J.M.V., 1993. A study of the glass transition of amylopectin-sugar mixtures. Polymer 34 (2), 346–358. https://doi.org/10.1016/0032-3861(93)90088-R.

Kawai, K., Hagiwara, T., Takai, R., Suzuki, T., 2005. Comparative investigation by two analytical approaches of enthalpy relaxation for glassy glucose, sucrose, maltose, and trehalose. Pharmaceut. Res. 22 (3), 490–495. https://doi.org/10.1007/s11095-004-1887-6.

Khem, S., Small, D.M., May, B.K., 2016. The behaviour of whey protein isolate in protecting *Lactobacillus plantarum*. Food Chem. 190, 717–723. https://doi.org/10.1016/j.foodchem.2015.06.020.

Khem, S., Woo, M.W., Small, D.M., Chen, X.D., May, B.K., 2015. Agent selection and protective effects during single droplet drying of bacteria. Food Chem. 166, 206–214. https://doi.org/10.1016/j.foodchem.2014.06.010.

Leslie, S.B., Israeli, E., Lighthart, B., Crowe, J.H., Crowe, L.M., 1995. Trehalose and sucrose protect both membranes and proteins in intact bacteria during drying. Appl. Environ. Microbiol. 61 (10), 3592–3597.

Lian, W.C., Hsiao, H.C., Chou, C.C., 2002. Survival of bifidobacteria after spray-drying. Int. J. Food Microbiol. 74 (1–2), 79–86. https://doi.org/10.1016/S0168-1605(01)00733-4.

Liu, B., Fu, N., Woo, M.W., Chen, X.D., 2018. Heat stability of *Lactobacillus rhamnosus* GG and its cellular membrane during droplet drying and heat treatment. Food Res. Int. 112 (May), 56–65. https://doi.org/10.1016/j.foodres.2018.06.006.

Nicolai, T., Britten, M., Schmitt, C., 2011. β-Lactoglobulin and WPI aggregates: formation, structure and applications. Food Hydrocolloids 25 (8), 1945–1962. https://doi.org/10.1016/j.foodhyd.2011.02.006.

Paramita, V., Iida, K., Yoshii, H., Furuta, T., 2010. Effect of additives on the morphology of spray-dried powder. Dry. Technol. 28 (3), 323–329. https://doi.org/10.1080/07373931003627098.

Peighambardoust, S.H., Golshan Tafti, A., Hesari, J., 2011. Application of spray drying for preservation of lactic acid starter cultures: a review. Trends in Food Science and Technology. https://doi.org/10.1016/j.tifs.2011.01.009.

Perdana, J., Bereschenko, L., Fox, M.B., Kuperus, J.H., Kleerebezem, M., Boom, R.M., Schutyser, M.A.I., 2013. Dehydration and thermal inactivation of *Lactobacillus plantarum* WCFS1: comparing single droplet drying to spray and freeze drying. Food Res. Int. 54 (2), 1351–1359. https://doi.org/10.1016/j.foodres.2013.09.043.

Perdana, J., Bereschenko, L., Roghair, M., Fox, M.B., Boom, R.M., Kleerebezem, M., Schutyser, M.A.I., 2012. Novel method for enumeration of viable *Lactobacillus plantarum* WCFS1 cells after single-droplet drying. Appl. Environ. Microbiol. 78 (22), 8082–8088. https://doi.org/10.1128/AEM.02063-12.

Perdana, J., Fox, M.B., Siwei, C., Boom, R.M., Schutyser, M.A.I., 2014. Interactions between formulation and spray drying conditions related to survival of *Lactobacillus plantarum* WCFS1. Food Res. Int. 56, 9–17. https://doi.org/10.1016/j.foodres.2013.12.007.

Ribeiro, C., Zimeri, J.E., Yildiz, E., Kokini, J.L., 2002. Estimation of effective diffusivities and glass transition temperature of polydextrose as a function of moisture content. Carbohydr. Polym. 51 (3), 273–280. https://doi.org/10.1016/S0144-8617(02)00182-0.

Sadek, C., Li, H., Schuck, P., Fallourd, Y., Pradeau, N., Le Floch-Fouéré, C., Jeantet, R., 2014. To what extent do whey and casein micelle proteins influence the morphology and properties of the resulting powder? Dry. Technol. 32 (13), 1540–1551. https://doi.org/10.1080/07373937.2014.915554.

Sadek, C., Tabuteau, H., Schuck, P., Fallourd, Y., Pradeau, N., Le Floch-Fouéré, C., Jeantet, R., 2013. Shape, shell, and vacuole formation during the drying of a single concentrated whey protein droplet. Langmuir 29 (50), 15606–15613. https://doi.org/10.1021/la404108v.

Santivarangkna, C., Aschenbrenner, M., Kulozik, U., Foerst, P., 2011. Role of glassy state on stabilities of freeze-dried probiotics. J. Food Sci. 76 (8) https://doi.org/10.1111/j.1750-3841.2011.02347.x.

Santivarangkna, C., Kulozik, U., Foerst, P., 2007. Alternative drying processes for the industrial preservation of lactic acid starter cultures. Biotechnol. Prog. 23 (2), 302–315. https://doi.org/10.1021/bp060268f.

Schutyser, M.A.I., Both, E.M., Siemons, I., Vaessen, E.M.J., Zhang, L., 2019. Gaining insight on spray drying behavior of foods via single droplet drying analyses. Dry. Technol. 37 (5), 525–534. https://doi.org/10.1080/07373937.2018.1482908.

Schutyser, M.A.I., Perdana, J., Boom, R.M., 2012. Single droplet drying for optimal spray drying of enzymes and probiotics. Trends in Food Science and Technology 27 (2), 73–82.

Siemons, I., Politiek, R.G.A., Boom, R.M., Sman, R.G.M., Der, Van, Schutyser, M.A.I., 2020. Dextrose equivalence of maltodextrins determines particle morphology development during single sessile droplet drying. Food Res. Int. 131, 108988. https://doi.org/10.1016/j.foodres.2020.108988. November 2019.

Vaessen, E.M.J., den Besten, H.M.W., Leito, K.M.N., Schutyser, M.A.I., 2020. Pulsed electric field pre-treatment for enhanced bacterial robustness during drying: Effect of carrier matrix and strain variability. Submitted for publication.

Vaessen, E.M.J., den Besten, H.M.W., Patra, T., van Mossevelde, N.T.M., Boom, R.M., Schutyser, M.A.I., 2018. Pulsed electric field for increasing intracellular trehalose content in *Lactobacillus plantarum* WCFS1. Innovat. Food Sci. Emerg. Technol. 47, 256–261. https://doi.org/10.1016/J.IFSET.2018.03.007.

van der Sman, R.G.M., Meinders, M.B.J., 2011. Prediction of the state diagram of starch water mixtures using the Flory-Huggins free volume theory. Soft Matter 7 (2), 429–442. https://doi.org/10.1039/c0sm00280a.

van der Sman, R.G.M., Meinders, M.B.J., 2013. Moisture diffusivity in food materials. Food Chem. 138 (2–3), 1265–1274. https://doi.org/10.1016/j.foodchem.2012.10.062.

Vehring, R., 2008. Pharmaceutical particle engineering via spray drying. Pharmaceut. Res. 25 (5), 999–1022. https://doi.org/10.1007/s11095-007-9475-1.

Vehring, R., Foss, W.R., Lechuga-Ballesteros, D., 2007. Particle formation in spray drying. J. Aerosol Sci. 38 (7), 728–746. https://doi.org/10.1016/j.jaerosci.2007.04.005.

Wang, J., Huang, S., Fu, N., Jeantet, R., Chen, X.D., 2016. Thermal aggregation of calcium-fortified skim milk enhances probiotic protection during convective droplet drying. J. Agric. Food Chem. 64 (30), 6003–6010. https://doi.org/10.1021/acs.jafc.6b02205.

Würth, R., Foerst, P., Kulozik, U., 2018. Effects of skim milk concentrate dry matter and spray drying air temperature on formation of capsules with varying particle size and the survival microbial cultures in a microcapsule matrix. Dry. Technol. 36 (1), 93–99. https://doi.org/10.1080/07373937.2017.1301952.

Yang, Z., Peng, H., Wang, W., Liu, T., 2010. Crystallization behavior of poly (ε-caprolactone)/layered double hydroxide nanocomposites. J. Appl. Polym. Sci. 116 (5), 2658–2667. https://doi.org/10.1002/app.

Zheng, X., Fu, N., Duan, M., Woo, M.W., Selomulya, C., Chen, X.D., 2015. The mechanisms of the protective effects of reconstituted skim milk during convective droplet drying of lactic acid bacteria. Food Res. Int. 76 (3), 478–488. https://doi.org/10.1016/j.foodres.2015.07.045.

Zobrist, B., Soonsin, V., Luo, B.P., Krieger, U.K., Marcolli, C., Peter, T., Koop, T., 2011. Ultra-slow water diffusion in aqueous sucrose glasses. Phys. Chem. Chem. Phys. 13 (8), 3514–3526. https://doi.org/10.1039/c0cp01273d.